2024-1408 IJOI
https://www.ijoi-online.org/

International Journal of Organizational Innovation

INFLUENCE OF SHEAR BANDING ON THE ACTIVE EARTH PRESSURE OF RETAINING WALLS

Tse-Shan Hsu
Founding President, Institute of Mitigation for Earthquake Shear Banding Disasters
Professor, Department of Civil Engineering, Feng-Chia University, Taiwan R.O.C.
tshsu@fcu.edu.tw

Hung-Chia Chang
Manager, Civil Engineering Maintenance Section, Maintenance Management Division,
Port of Taichung, Taiwan Internation Port Corp. LTD., Taiwan, R.O.C.

Abstract

Engineers commonly rely on the Rankine active earth pressure formula, as prescribed in design codes, when designing retaining walls. However, research has demonstrated that retaining walls designed using this approach may be prone to failure under conditions such as heavy rainfall, earthquakes, or even under normal scenarios without wind, rain, or seismic activity. To address this issue, the present study uses the pier caisson-type retaining wall at the Taichung Port in Taiwan, as a case study to investigate the influence of shear banding on the active earth pressure exerted on retaining walls. The key findings are as follows: (1) During significant lateral displacement of the retaining wall toward the seaward side, the soil behind the wall undergoes lateral unloading; as the Mohr circle expands and tangentially intersects the yield envelope, the soil reaches its yield point and enters the plastic range. (2) In a plastic strain-softening model, shear band failure planes develop in the soil behind the wall. In contrast, no such failure planes are observed in a perfectly plastic model. This suggests that soil yielding does not always lead to the formation of shear band failure planes. (3) Significant lateral movement of the retaining wall is required to induce active earth pressure, it is crucial to account for the residual shear strength parameters of the soil, which are determined once strain has sufficiently pene-

trated the plastic range. Based on these findings, the authors recommend integrating shear banding theory and the corresponding active earth pressure calculation formulas into future design codes to enhance the stability of retaining walls.

Keywords: caisson, retaining wall, shear band, soil liquefaction, strain softening.

Introduction

In 1995, Japan was struck by the 7.2 magnitude Hanshin earthquake. The measured horizontal peak ground acceleration at the Kobe Port pier caisson was 0.55g, and the maximum lateral displacement toward the sea was 5.9 meters, resulting in significant damage (Figure 1). Similarly, in 1999, Taiwan experienced the 7.3 magnitude Jiji earthquake. The measured horizontal peak ground acceleration at the Taichung Port pier caisson, located 50 kilometers from the epicenter, was 0.163g. The maximum lateral displacement of the pier caisson-type retaining wall was 1.7 meters, causing substantial damage (Figure 2).

Figure 1. Damage to the rear line region of the pier caisson caused by the 1995 Great Hanshin Earthquake, Kobe Port, Japan (Kobe Geotechnical Collection, 2019).

Figure 2. Damage to the rear line region of the pier caisson caused by the 1999 Jiji Earthquake, Taichung Port, Taiwan (Lai et al., 2007).

The pier caisson-type retaining wall at the Taichung Port in Taiwan is 19.2 meters high, with a water depth of 13.2 meters on the seaward side and an elevation of 6.2 meters at the rear line region. The failures observed during both the Hanshin and Jiji earthquakes clearly suggest that the active earth pressure formula used in the design codes was likely applied without considering the effects of shear banding in the rear line region of the wall. This oversight may have led to an underestimation of the active earth pressure acting on the retaining wall. Therefore, it is essential to revise the active earth pressure formula in the design codes to accurately account for the impact of shear banding.

Issues Arising from the Active Earth Pressure Formula Provided by the Design Codes

The active earth pressure formula, as shown in Equation (1), provided in the current design codes for building foundation structures (2023) for retaining walls—particularly for soils with both cohesion (c) and internal friction angle (ϕ)—has several limitations due to the assumptions made during its derivation. Based on Rankine's theory (McCarthy, 1977), this formula assumes that the soil behaves as an elastic-perfectly plastic material, with no wall friction angle ($\delta = 0$) and other simplifications that fail to accurately represent the true behavior of cohesive-frictional (c-ϕ) soils.

$$P_a = \frac{1}{2}\gamma H^2 \tan^2\left(45^\circ - \frac{\phi}{2}\right) - 2cH\tan\left(45^\circ - \frac{\phi}{2}\right) \quad (1)$$

For Equation (1), the assumptions made by Rankine (1857) in deriving the formula, as illustrated in Figure 3, include:

1. The soil is modeled as an elastic-perfectly plastic material.
2. The yield envelope is used as the Mohr-Coulomb failure envelope.
3. The wall friction angle (δ) is assumed to be zero.
4. The soil behind the wall is assumed to be non-cohesive, dry, and to have a slope angle of β.
5. The active earth pressure acting on the retaining wall is assumed to be equivalent to the pressure exerted by an infinitely extending, uniform soil slope.
6. The direction of the active earth pressure is assumed to be parallel to the slope.

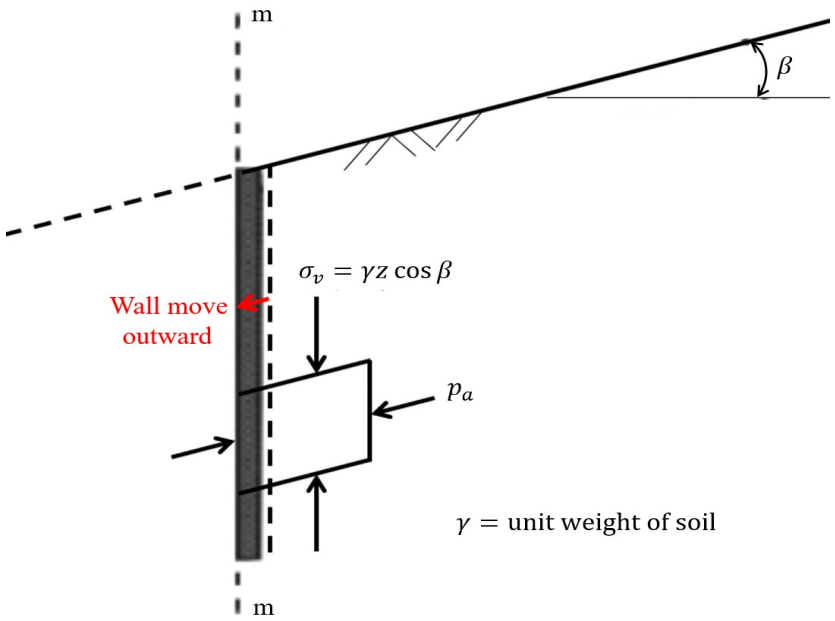

Figure 3. Basic elements of Rankine's active earth pressure theory (McCarthy, 1977).

For a cohesive-frictional (c-ϕ) soil stratum, it is important to recognize that the actual soil behaves as an elastic-plastic strain-softening material (Hsu, 1987; Hsu, 2022). Under the six assumptions made by Rankine, the yielding of a perfectly plastic soil only indicates that the soil has entered the

plastic range, without necessarily resulting in the formation of failure planes. Additionally, the wall friction angle ($\delta \neq 0$) is present due to the c-ϕ soil behind the retaining wall. Therefore, the first three assumptions made by Rankine do not fully reflect the actual conditions. Consequently, directly applying Equation (1) to calculate the active earth pressure on the retaining wall introduces uncertainties that may compromise the safety of the wall.

Figure 4 illustrates a schematic cross-section of the pier caisson-type retaining wall and the soil layers behind it at Taichung Port, Taiwan. In this diagram, the retaining wall has a vertical back, and the surface of the soil behind the wall is horizontal. Figure 5 shows the Mohr circle for an element at depth z, subjected to the maximum principal stress (σ_1) and the minimum principal stress (σ_3), where σ_1 represents the vertical stress and σ_3 represents the horizontal stress.

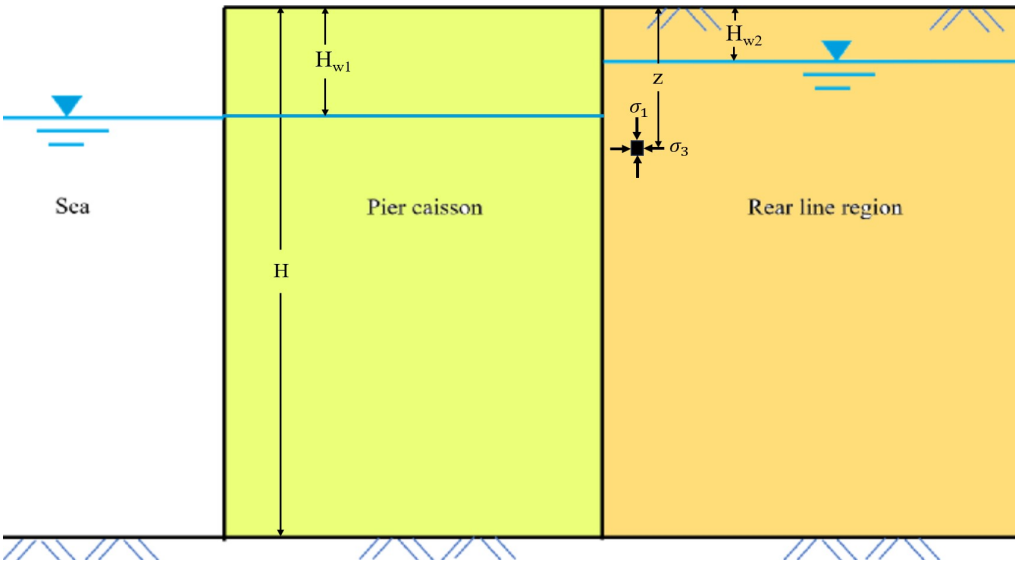

Figure 4. Schematic diagram showing the maximum and minimum principal stresses acting on an element within the soil layer behind the pier caisson-type retaining wall at Taichung Port, Taiwan.

As the pier caisson-type retaining wall, shown in Figure 4, moves toward the sea, Figure 5 illustrates the expansion of the Mohr circle due to the reduction in lateral earth pressure. As the Mohr circle expands and becomes tangent to the yield envelope, the minimum principal stress (σ_3) acting on the soil element decreases to the minimum principal stress under yield conditions (σ_{3y}). At this point, the element in the soil layer yields and enters the plastic range.

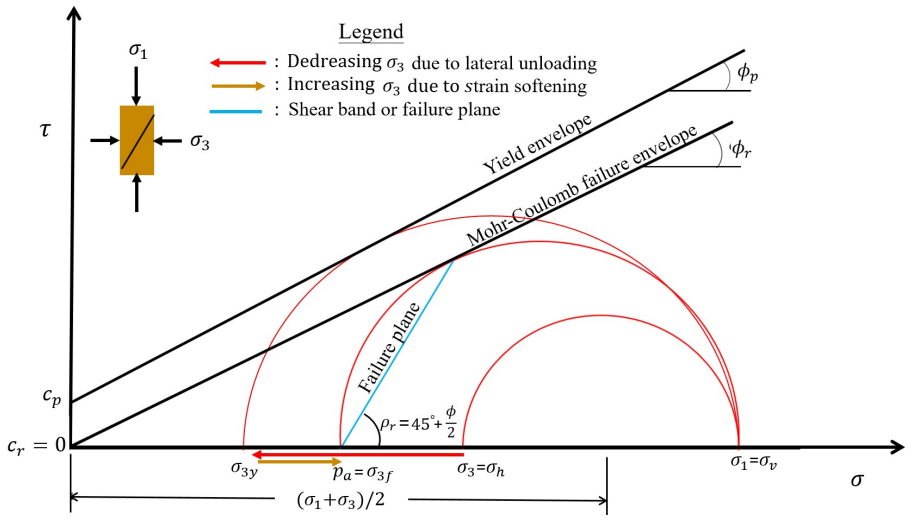

Figure 5. Mohr's circle representing the principal stresses (σ_1 and σ_3) acting on an element in the soil layer behind the retaining wall.

Within the plastic range, Hsu (2022) demonstrated that the perfectly plastic model is stable, while the plastic strain-softening model is unstable. Hsu (1987, 2022) also showed that only the unstable plastic strain-softening model leads to the formation of shear band failure planes as strain progresses deeper into the plastic range. Therefore, in Figure 5, the shear band failure planes appear only when the Mohr circle is tangent to the Mohr-Coulomb failure envelope, not when it is tangent to the yield envelope.

In direct shear test results, the yield envelope is derived from the peak strength values of the stress-strain curves obtained from tests on three specimens, providing the experimental values of peak cohesion (c_p) and peak friction angle (ϕ_p). In contrast, the Mohr-Coulomb failure envelope is obtained from the residual strength values

of the stress-strain curves for the same specimens, yielding the experimental values of residual cohesion (c_r) and residual friction angle (ϕ_r).

Active Earth Pressure Formula for Retaining Walls Considering Shear Banding Effects

For the pier caisson-type retaining wall at Taichung Port in Taiwan, as shown in Figure 6, a Coulomb wedge sliding failure block (Coulomb, 1773/1776) is generated when the retaining wall moves toward the sea along line $\overline{BM}$. In this case, segments $\overline{AB}$ and $\overline{CB}$ represent the shear band failure surfaces. When the retaining wall is subjected to Coulomb active earth pressure, the shear band failure planes $\overline{AB}$ and $\overline{CB}$ of the wedge block $\Delta\overline{ABC}$ experience plastic strain softening, while the regions outside these shear band failure planes remain in an elastic strain state.

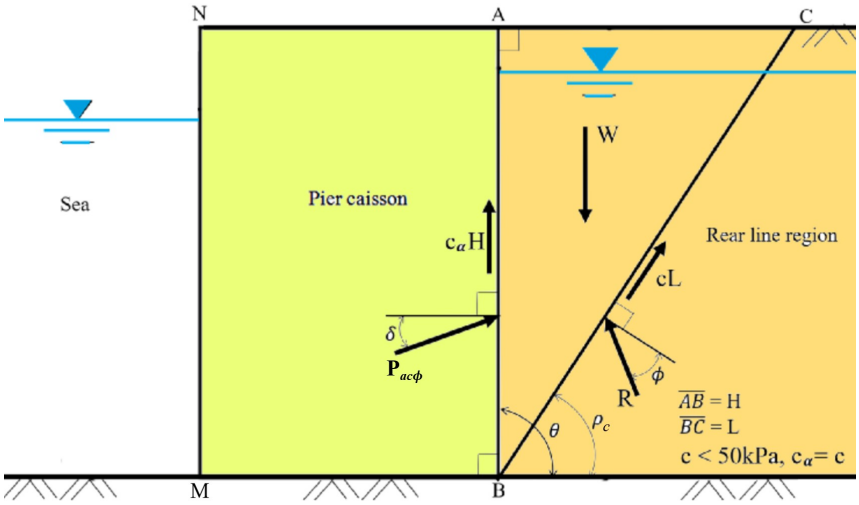

Figure 6. Various forces and the active earth pressure acting on the pier caisson-type retaining wall at Taichung Port, Taiwan, along with the wedge failure block in the region behind the wall.

Calculation Formula for Active Earth Pressure $P_{a\phi}$ of Frictional Soil

When the backfill soil behind a retaining wall is frictional, the gravitational force W of the Coulomb wedge sliding failure block $\Delta\overline{ABC}$, as shown in Figure 6, can be calculated as follows:

$$W = \frac{1}{2}\gamma \overline{BC} \cdot \overline{AB} \cdot sin(\theta - \rho_{c0})$$
$$= \frac{1}{2}\gamma H^2 \frac{sin(\theta-\beta)}{sin^2\theta} \cdot \frac{sin(\theta-\rho_{c0})}{sin(\rho_{c0}-\beta)} \quad (2)$$

In Equation (2), $\overline{AB}$ represents the back of the retaining wall, and $\overline{CB}$ represents the sliding failure plane of the wedge-shaped block. Figure 7 shows the force polygon of the three forces W, R, and $P_{a\phi}$. When these forces are balanced, the force polygon is closed.

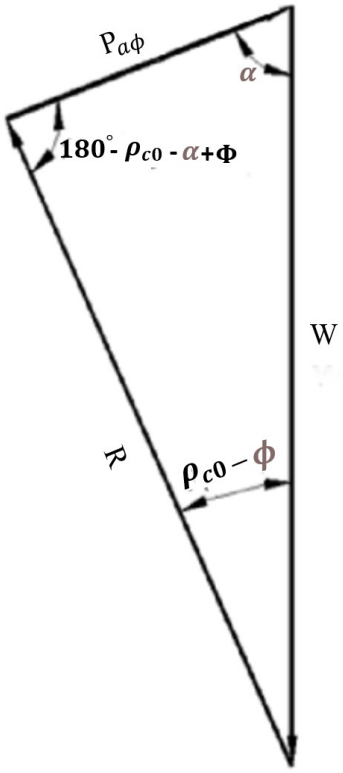

Figure 7. The closed force polygon of *W*, *R*, and $P_{a\phi}$.

According to the law of sines, the active earth pressure $P_{a\phi}$ shown in Figure 7 for frictional soils can be determined as follows:

$$P_{a\phi} - W\frac{sin(\rho_c - \phi)}{sin(180^\circ - \rho_c - \alpha + \phi)} = \frac{1}{2}\gamma H^2 \frac{sin(\theta-\beta)}{sin^2\theta} \cdot \frac{sin(\theta-\rho_c)}{sin(\rho_c-\beta)} \cdot \frac{sin(\rho_c-\phi)}{sin(\rho_c+\alpha-\phi)} \quad (2)$$

For the failure wedge shown in Figure 6, the active earth pressure $P_{a\phi}$ for frictional soils can also be expressed as:

$$P_{a\phi} - \frac{1}{2}\gamma H^2 K_{a\phi} \quad (3)$$

where $K_{a\phi}$ is the coefficient of active earth pressure $P_{a\phi}$ for frictional soils. It is defined as:

$$K_{a\phi} = \frac{sin(\theta-\beta)}{sin^2\theta} \cdot \frac{sin(\theta-\rho_{c0})}{sin(\rho_{c0}-\beta)} \cdot \frac{sin(\rho_{c0}-\phi)}{sin(\rho_{c0}+\alpha-\phi)} \quad (4)$$

By adjusting the inclination angle of the sliding failure plane such that $P_{a\phi}$ in Equation 2 is the maximum value. Therefore, if and only if active earth pressure function shown in Equation 2 exists, then Equation 5 was proved by Hsu et al. (2021) as the governing equation for solving active earth pressure $P_{a\phi}$ for frictional soils.

$$cot(\theta - \rho_{c0}) + cot(\rho_{c0} - \beta) = cot(\rho_{c0} - \phi) - cot(\rho_{c0} + \alpha - \phi) \quad (5)$$

When the values of θ, β, ϕ, and α are known, solving Equation (5) will yield ρ_{c0}. Then, by substituting ρ_{c0} into Equations (2) and (4), the active earth pressure $P_{a\phi}$ and the active earth pressure coefficient $K_{a\phi}$ for frictional soil can be determined, respectively.

Calculation Formula for Active Earth Pressure $P_{ac\phi}$ of c-ϕ Soil

When the retaining wall is backed by cohesive-frictional (c-ϕ) soil, the active earth pressure acting on the wall consists not only of the frictional component but also includes contributions from the cohesive force cL and adhesive force $c_\alpha H$, as shown in Figure 7. Therefore, the active earth pressure $P_{ac\phi}$ of cohesive-frictional (c-ϕ) soil exerted on the retaining wall can be calculated as follows:

$$
\begin{aligned}
c\mathrm{L} &= c\,\overline{\mathrm{CB}} \\
&= c\,\overline{\mathrm{AB}}\sin\left(180^\circ - \theta + \beta\right)/\sin(-\beta) \\
&= c\mathrm{H}\sin\left(180^\circ - \theta + \beta\right)/\left[\sin\left(180^\circ - \theta\right)\sin\left(\rho_c - \beta\right)\right]
\end{aligned} \tag{6}
$$

Figure 7 shows the force polygon of the five forces W, R-ΔR, cL, c_αH, and $\mathrm{P}_{ac\phi}$ in Figure 6. When the forces are balanced, the force polygon is closed.

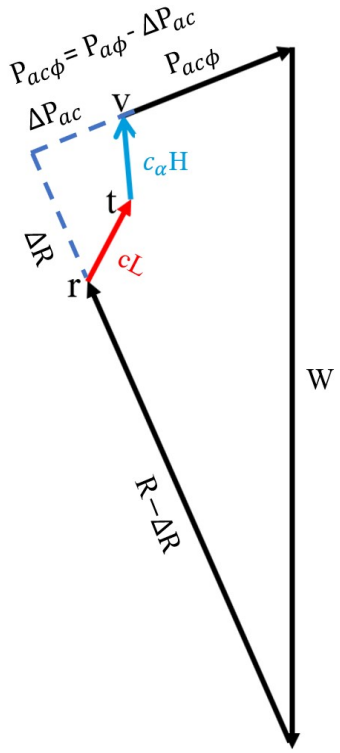

Figure 7. The closed force polygon of *W*, R-ΔR, cL, c_αH, and $\mathrm{P}_{ac\phi}$.

The lower triangle in Figure 8 shows the force polygon formed by ΔP_{ac1}, ΔR_1, and cL, while the upper triangle shows the force polygon formed by ΔP_{ac2}, ΔR_2, and c_αH. When the forces are balanced, both the upper and lower force polygons are closed.

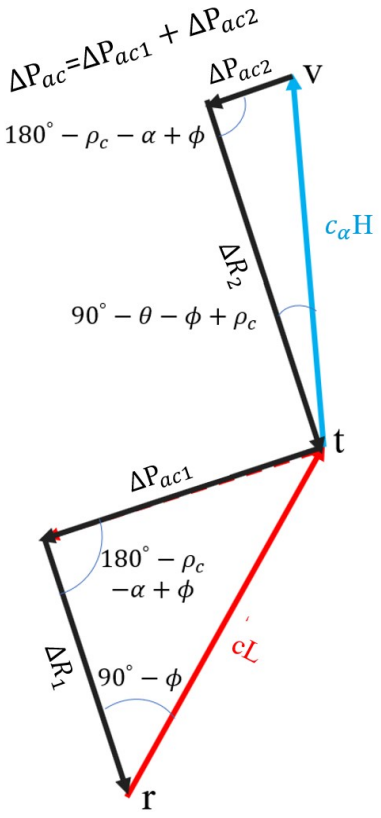

Figure 8. The closed lower triangle force polygon formed by cL, $\Delta P_{ac1}, \Delta R_1$ and the closed upper triangle force polygon formed by c_αH , $\Delta P_{ac2}, \Delta R_2$.

Based on Figures 7 and 8, the active earth pressure ($P_{ac\phi}$) for cohesive-frictional (c-ϕ) soil is determined as follows:

$$P_{ac\phi} = P_{a\phi} - \Delta P_{ac} = P_{a\phi} - \Delta P_{ac1} - \Delta P_{ac2} \quad (8)$$

Therefore, the active earth pressure coefficient ($K_{ac\phi}$) for cohesive-frictional (c-ϕ) soil is calculated as follows:

$$K_{ac\phi} = 2P_{ac\phi}/(\gamma H^2) \quad (9)$$

Figure 8 shows the closed force polygons required to calculate the active earth pressure increments ΔP_{a1} and ΔP_{a2}, corresponding to the cohesive force (cL) and adhesive force (c_αH), respectively. By applying the sine rule to the lower triangle in Figure 8, we can obtain:

$$\Delta P_{ac1} = \mathrm{cL}\frac{\sin(90^\circ-\phi)}{\sin(180^\circ-\rho_c-\alpha+\phi)}$$

$$= \mathrm{cH}\frac{\sin(\theta-\beta)\cdot\cos\phi}{\sin(\theta)\cdot\sin(\rho_c-\beta)}\cdot\frac{1}{\sin(\rho_c+\alpha-\phi)}$$

$$= \mathrm{cH}\frac{\sin(\theta-\beta)\cdot\cos\phi}{\sin(\theta)}\cdot\left[\frac{1}{\sin(\rho_c-\beta)\cdot\sin(\rho_c+\alpha-\phi)}\right] \quad (10)$$

Additionally, by applying the sine rule to the upper triangle shown in Figure 8, we can obtain:

$$\Delta P_{ac2} = \mathrm{c}_\alpha\mathrm{H}\frac{\sin(90^\circ+\rho_c-\theta-\phi)}{\sin(180^\circ-\rho_c-\alpha+\phi)} = \mathrm{c}_\alpha\mathrm{H}\frac{\sin(90^\circ+\rho_c-\theta-\phi)}{\sin(\rho_c+\alpha-\phi)} \quad (11)$$

Case Study

For the cohesive-frictional (c-ϕ) soil in the rear line region of the pier caisson-type retaining wall at Taichung Port in Taiwan, Figure 9 presents the results from a direct shear test conducted on field-sampled specimens in the laboratory. From Figure 9, it is evident that the peak cohesion (c_p=10.2kPa), the peak internal friction angle (ϕ_p=36°), the residual cohesion (c_r=0 kPa), and the residual internal friction angle (ϕ_r=30 °) are observed.

For the pier caisson-type retaining wall at the Taichung Port in Taiwan shown in Figure 6 with a height H=19.2 m, the inclination angle of the wall face $\overline{AB}$ is $\theta = 90^\circ$, while the inclination angle of the ground surface $\overline{AC}$ in the rear line region is $\beta = 0^\circ$, and the unit weight of the soil is $\gamma = 20\,kN/m^3$.

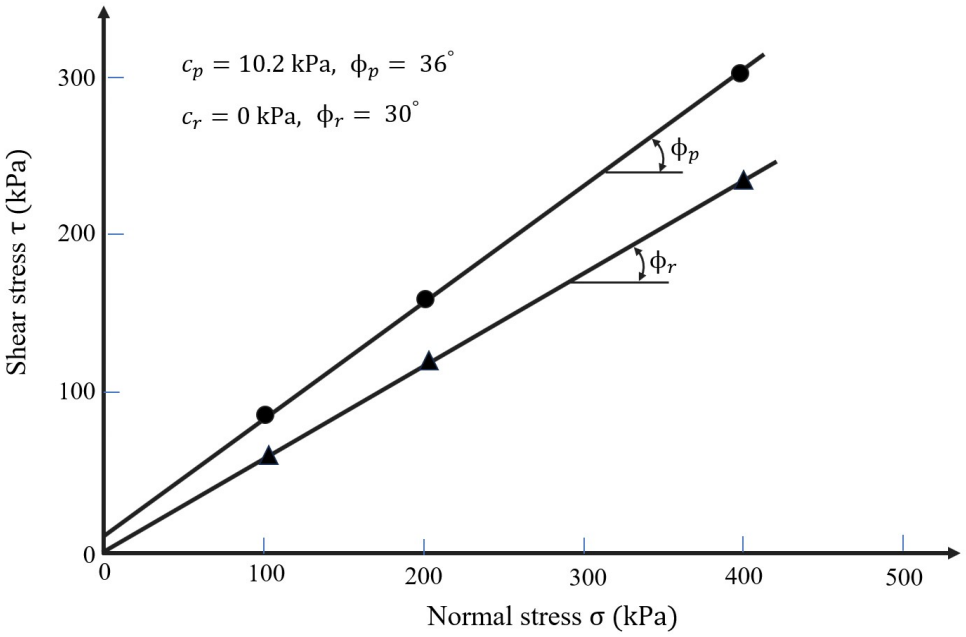

Figure 9. The direct shear test results of the c-ϕ soils from the rear line region of the pier caisson at the Taichung Port in Taiwan

Case 1: Calculation of Active Earth Pressure on the Retaining Wall Using Formulas Provided by the Codes

For the cohesive-frictional (c-ϕ) soil in the rear line region of pier caisson-type retaining wall at the Taichung Port in Taiwan, the Foundation Structure Design Code (2023) provides the following Rankine formula for calculating the active earth pressure (P_a) on the retaining wall.

$$P_a = \frac{1}{2}\gamma H^2 \tan^2\left(45^\circ - \frac{\phi}{2}\right) - 2cH\tan\left(45^\circ - \frac{\phi}{2}\right) \quad (14)$$

Since the perfectly plastic model was adopted by Rankine in the derivation of Equation 14, when applying Equation 14 to calculate the active earth pressure, it is necessary to use the peak cohesion ($c_p = 10.2$ kPa), and the peak internal friction angle ($\phi_p = 36^\circ$), and the wall friction angle ($\delta = 0^\circ$).. Therefore, the inclination angle of the sliding failure surface (ρ_c), the active

earth pressure coefficient (K_a), and the active earth pressure (P_a) can be calculated as follows:

$$\rho_c = 45^\circ + \frac{36^\circ}{2} = 63^\circ,$$

$$K_a = \tan^2\left(45^\circ - \frac{36^\circ}{2}\right) = 0.2596,$$

$$P_a = \frac{1}{2} \cdot 0.2596 \cdot 20 \cdot 19.2^2 - 2 \cdot 10.2 \cdot 19.2 \cdot \sqrt{0.2596} = 757.48\text{kPa}.$$

Case 2: Calculation of Active Earth Pressure on Retaining Wall Using the Formula Proposed by the Authors

In this paper, the authors present Formulas (8) and (9) to calculate the active earth pressure ($P_{ac\phi}$) acting on retaining walls for cohesive-frictional (c-ϕ) soil. Since the soil has entered the plastic range when the active earth pressure is induced, it is in a state of plastic strain softening. Therefore, in the calculation of active earth pressure, the soil parameters used should correspond to those after plastic strain softening, specifically the residual cohesion ($c_r = 0$ kPa), residual internal friction angle ($\phi_r = 30^\circ$), and wall friction angle ($\delta = 21.05^\circ$).

In this case study, the inclination angle of the sliding failure surface (ρ_c=55.8º) is first determined using Equation (8). Subsequently, the active earth pressure ($P_{a\phi} = 1094.13$ kPa), along with the active pressure differences caused by cohesive force (ΔL =0kPa) and adhesive force (c_αH =0kPa), can be calculated using Equations (10) and (11), resulting in the active earth pressure increment ΔP_{ac1}= 0kPa, and the active earth pressure increment ΔP_{ac2}=0 kPa, respectively. Thus, the active earth pressure ($P_{ac\phi}$) and the active earth pressure coefficient ($K_{ac\phi}$) can be determined as follows:

$$P_{ac\phi} = P_{a\phi} - \Delta P_{ac1} - \Delta P_{ac2} = 1094.13 \text{ kPa},$$

$$K_{ac\phi} = \frac{2P_{ac\phi}}{\gamma H^2} = 0.2968$$

Comparison and Discussion

1. For the retaining wall shown in Figure 10, the derivation of the Rankine active earth pressure formula is based on the following six assumptions (Rankine, 1856):
   (a) An elastic-perfectly plastic soil model is adopted.
   (b) The Mohr-Coulomb failure envelope is adopted as the yield function.
   (c) The wall friction angle is assumed to be $\delta = 0$.
   (d) The slope of the soil on the back of the wall is β of frictional dry backfill.
   (e) The active earth pressure of the retaining wall is the earth pressure of an infinitely extending uniform soil slope.
   (f) The direction of the active earth pressure is assumed parallel to the slope.

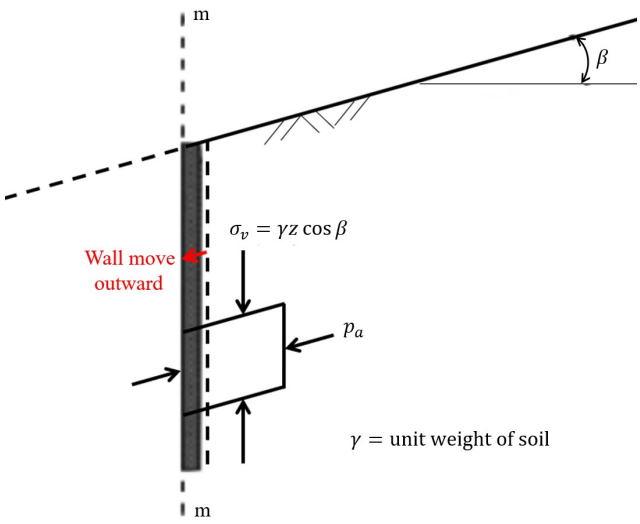

Figure 10 Basic elements of Rankine active earth pressure (Reproduced from McCarthy, 1977).

2. After the strain has entered the plastic range, the soil strength decreases from peak strength to residual strength. However, the Rankine active earth pressure theory adopts a perfectly plastic model without considering the effect of plastic strain softening.

3. For the perfectly plastic model adopted in Rankine's active earth pressure theory, the inner product of the stress increment tensor ($d\boldsymbol{\sigma}$) and the strain increment tensor ($d\boldsymbol{\varepsilon}$) is zero. Therefore, based on Drucker's stability postulate, it is known that the perfectly plastic model is stable.

4. Since actual soils exhibit plastic strain softening behavior, in this case, the inner product of the stress increment tensor ($d\boldsymbol{\sigma}$) and the strain increment tensor ($d\boldsymbol{\varepsilon}$) is less than zero. According to Drucker's stability postulate, it is known that the plastic strain softening model is unstable.

5. Hsu et al. (1987 and 2022) demonstrated that in a stable perfectly plastic model, no shear band failure surface is formed once the strain enters the plastic range. However, in an unstable plastic strain-softening model, shear band failure planes develop as the strain progresses deeper into the plastic range.

6. When a retaining wall is subjected to active earth pressure, shear band failure planes develop in the soil behind the wall. Therefore, in deriving the active earth pressure formula for the retaining wall, the stable perfectly plastic model should be avoided. Instead, the unstable plastic strain-softening model should be adopted. In Rankine's derivation of the active earth pressure formula, both the unstable sliding failure surface and the stable perfectly plastic model are applied simultaneously. As a result, these incompatible conditions lead to an active earth pressure formula that does not align with practical requirements.

7. For the pier caisson-type retaining wall at Taichung Port in Taiwan, the active earth pressure is closely linked to the shear band failure planes. The actual active earth pressure, based on the shear band failure plane, is 1094.13 kPa. However, previous researchers and engineers have typically used the formula provided in design codes, which is based on the yield envelope. As a result, the active earth pressure calculated using the design code formula is only 757.48 kPa. In

other words, the actual active earth pressure, which represents the maximum value, is 44.4% higher than the value obtained using the design code.

8. Since there is often a difference in the water tables on both sides of the pier caisson, placing the pier caisson directly on the seabed can cause the hydraulic gradient (i) at the groundwater exit point M, as shown in Figure 5, to exceed the critical hydraulic gradient (i_c), leading to piping failure. During this failure process, the pier caisson will shift significantly toward the sea, resulting in substantial subsidence in the rear line region. This movement can also trigger sand boiling and soil liquefaction (Hsu, et al., 2017), particularly in the soil layers affected by shear banding and shear texturing (Figure 2).

Conclusions and Recommendations

Over the past two decades, many retaining walls in Taiwan have failed during heavy rainfall, earthquakes, and even under normal conditions (without wind, rain, or earthquakes). Engineers typically design retaining walls using the Rankine active earth pressure formula from the design codes, and post-disaster investigations often attribute these failures to poor construction quality. In this paper, the authors examine the pier caisson-type retaining wall at Taichung Port in Taiwan to investigate the causes of excessive active earth pressure acting on the wall. The research leads to the following three conclusions:

1. The pier caisson-type retaining wall at Taichung Port in Taiwan experienced active earth pressure due to significant movement toward the sea. This caused the soil behind the wall to enter the plastic strain range, where plastic strain softening contributed to the formation of shear band failure planes.

2. Hsu (2023) demonstrated that only an unstable plastic strain-softening model can induce the formation of shear band failure planes, while a stable perfectly plastic model cannot. As a result, Rankine's application of the stable perfectly plastic model in deriving the active earth pressure formula led to a fundamental misjudgment, assuming the

existence of shear band failure planes that do not actually form. Consequently, the Rankine formula fails to capture the maximum lateral earth pressure, leading to an underestimation of the active earth pressure acting on the retaining wall.

3. The active earth pressure calculated using the formula provided by the design code underestimated the actual pressure by 44.4%. As a result, the pier caisson-type retaining wall at Taichung Port in Taiwan experienced significant movement toward the sea. This movement not only caused substantial subsidence in the rear line region but also triggered localized sand boiling, soil liquefaction, and the formation of large piping holes.

Based on the three conclusions outlined above, the authors recommend that future retaining wall design codes incorporate the revised active earth pressure theory and calculation formulas presented in this paper. Furthermore, it is essential to clearly define the testing methods and results necessary for accurately calculating active earth pressure when designing retaining walls. By adopting these revisions, engineers will be better equipped to precisely determine the active earth pressure acting on retaining walls and design more stable structures that meet the desired performance objectives.

References

Chang, Hong-Chia, *A Study of the Major Cause for the 2018 Hualien Earthquake Disasters*, Ph.D. Dissertation, Advisor: Professor Dr. Tse-Shan Hsu, Feng-Chia University, Taiwan, 2019

Coulomb, C. A., "Essai sur une application des règles des Maximis et Minimis à quelques Problèmes de statique relatifs à l'Architecture," In: *Mémoires de mathématique & de physique, présentés à l'Académie Royale des Sciences par divers savans*, Vol. 7, 1773, pp. 343-382. Paris, 1773/1776

Hsu, Tse-Shan, *Capturing Localizations in Geotechnical Failures*, Ph. D. Dissertation, Civil Engineering in the School of Advanced Studies of Illinois of Technology, 1987

Hsu, Tse-Shan, *Plasticity Model Required to Prevent Geotechnical Failures in Tectonic Earthquakes*, A Chapter in "Earthquakes–Recent Advance, New

Perspectives and Applications," Edited by Walter Salazar, InteChOpen, pp. 101-121, 2022

Hsu, Tse-Shan, Chang-Chi Tsao, and Chihsen T. Lin, "Localizations of Soil Liquefactions Induced by Tectonic Earthquakes," *The International Journal of Organizational Innovation,* Vol.9, No. 3, Section C, pp. 110-131, 2017

Hsu, Tse-Shan, Yi-Ju Chen, Zong-Lin Wu, Yi-Lang Hsieh, Jiann-Cherng Yang, Yi-Min Huang, "Influence of Strain Softening and Shear-band Tilting Effect on the Maximum Earth Pressure of Retaining Walls," *International Journal of Organizational Innovation,* Vol. 14, No. 1, pp. 45-86, 2021

Kobe Geotechnical Collection, Earthquake Engineering Research Center, University of California, Berkeley, 2019

Lai, R. Y., Lai, S. Y., Hsieh, M. Z., & Lin, Y. W., *Study on the impact of liquefaction on the stability of port structures* (2/4), Transportation Research Institute, Ministry of Transportation and Communications, 96-22-7274, MOTC-IOT-94-H1DA002-3, 2007

McCarthy, D. F., *Essentials of Soil Mechanics and Foundations*, 7th Edition, New Jersey, Prentice Hall, p. 399, 1977.

Ministry of Interior, R.O.C., "Design Code and Specifications of Building Foundation Structures," 2023

Rankine, W., "On the stability of loose earth," Philosophical Transactions of the Royal Society of London, Vol. 147, 1857.